Observation of surface enhanced multiphoton photoemission from metal surfaces in the short pulse limit

M. Aeschlimann,[a] C. A. Schmuttenmaer,[b] H. E. Elsayed-Ali,[c] and R. J. D. Miller
Center for Photoinduced Charge Transfer, Department of Chemistry, University of Rochester, Rochester, New York 14627

J. Cao and Y. Gao
Department of Physics and Astronomy, University of Rochester, Rochester, New York 14627

D. A. Mantell
Xerox Webster Research Center, Webster, New York 14580

(Received 5 December 1994; accepted 22 February 1995)

Photoelectrons with excess kinetic energy corresponding to several absorbed photons above the work function have been measured from atomically clean Cu(110) and Cu(100) surfaces under ultrahigh vacuum conditions. The power dependence of the photoemission yield does not follow a simple power law dependence corresponding to the number of photons absorbed. This behavior is reminiscent of other above threshold ionization (ATI) or tunnel ionization (TI) processes observed for atoms in the gas phase. The photoelectrons are generated with laser pulsewidths less than 100 fs in duration and peak powers as low as 100 MW/cm^2. These intensities are on the order of 10^5 times lower than that required to observe similar phenomena in the gas phase. The relatively low intensities and correlation with surface roughness suggests a contribution from a surface enhancement mechanism. Thermal heating and space charge effects have been ruled out, and the possibility of electric field enhancement at the surface due to the coupling of photons into surface plasmons is discussed. The nonlinear yield and enhancement of the photoemission produced by short pulse excitation needs to be considered when discussing photoinduced hot electron reaction channels at metal surfaces. © *1995 American Institute of Physics.*

INTRODUCTION

There exists a great body of research on the topic of above threshold ionization (ATI) of isolated atoms in the gas phase. Briefly, ATI is a multiphoton process in which an atom absorbs more photons than the minimum necessary for ionization.[1] With laser intensities in the 10^{13}–10^{14} W/cm^2 range, as many as 40 peaks, have been reported in the electron energy distribution.[2] The number of review articles on this topic is evidence of the experimental and theoretical interest in this phenomenon.[3,4] Despite the great amount of interest in gas phase ATI, comparatively little has been done to date concerning ATI at solid surfaces, often called above threshold photoemission (ATP).[5]

Our work is motivated by the desire to use current ATI theories to understand the more complicated behavior observed at a metal surface. Several new considerations arise as a result of the solid state medium. ATI spectra can show peaks due to resonances induced by the AC Stark shift arising from the enormous light field (excited bound states are shifted into resonance with an intermediate number of photons). In a metal, however, the continuum band structure prohibits any sharp features, and only AC Stark shifts into resonance with surface states and image states[5] can produce sharp features in the photoelectron spectrum. On the other hand, since the occupied density of states in a metal has a sharp cutoff at the Fermi energy, it is possible to measure a series of plateaus, rather than peaks, separated by the photon excitation energy. One intriguing possibility present during ATP that is not allowed in ATI is that there can be significant field enhancement at the surface caused by surface plasmons, image states, and/or adsorbate induced dipole fields.

A few recent studies in which the classic ATP behavior of multiple peaks or plateaus separated by the incident photon energy in their photoelectron spectrum from a metal surface have been reported.[5–7] All these previous studies employ relatively high pulse energy (>100 μJ/cm^2/pulse) or peak intensity (>10 GW/cm^2) laser pulses. Together with the relatively long pulse durations involved, it is difficult to be sure that these results are not influenced by space charge effects, i.e., energy gained during the field-free Coulomb explosion of the electron cloud on the way from the sample to the detector.[8]

In this paper we present the first observation of ATP spectra from single crystal copper surfaces in the ''very short'' pulse regime, where very short refers to pulse durations less than ~500 fs (Ref. 3), and we also provide analogies with ATI and tunnel ionization (TI) experiments. Using pulse durations less than 100 fs, the electrons are produced with the kinetic energy possessed at the moment of photoemission, rather than the value that they would attain in a ''long pulse'' (pulse duration greater than ~0.5 ps) measurement, where the electrons can acquire significant amounts of the quiver energy back from the light field due to pondero-

[a]Present address: Laboratory for Technical Chemistry, ETH Zurich, 8092 Zurich, Switzerland.
[b]Present address: Department of Chemistry, Yale University, 225 Prospect St., New Haven, Connecticut 06520.
[c]Present address: Department of Electrical Engineering and Computer Science, Old Dominion University, Norfolk, Virginia 23529.

 0021-9606/95/102(21)/8606/8/$6.00

motive acceleration.[4] Furthermore, we ensure that the average number of electrons emitted per pulse is on the order of one in order to avoid space charge effects as discussed by Petite *et al.*[8] In the present study, electrons with as much as 7 eV kinetic energy have been measured. The present work is unique in that far lower laser pulse energy and peak intensity are used in this study than in previous work. This allows us to rule out several possible competing mechanisms, such as space charge acceleration, transient thermionic emission, and ponderomotive acceleration. Finally, it is necessary to find rough spots on the surface when using these low intensities, which indicates that surface roughness plays a critical role in this process.

Apart from the intrinsic interest in the surface–laser field interaction that leads to electrons with large excess energy, there are also important surface photochemical issues on which these observations may have an impact. Many photoprocesses at metal surfaces have been considered to be thermal in nature (i.e., simple laser heating of the lattice), especially when employing high intensity pulsed lasers.[9] There has been an increasing amount of evidence that many of these processes are due to electronic excitations, however.[9] Recently, a great deal of attention has been paid to nonthermal photoinduced reactions in which vibrationally and rotationally hot desorption products are observed. These have been observed for one-photon as well as multiphoton excitation. In either case, excited electrons are believed responsible for the reactions.[10–12]

These new observations of true surface photochemistry are generally interpreted as arising from subvacuum electrons within the metal that couple to excited states of adsorbates at the metal surface. The electronic reaction channel in multiphoton processes is separable from thermal mechanisms only when short pulses are utilized, that is, on time scales shorter than lattice heating from the photoexcited electrons. For one-photon processes, the electronic and thermal contributions can be separated by using very low intensity illumination,[13] but for processes that have a superlinear fluence dependence, or when time resolved studies are carried out with short pulsewidths (<1 ps), it is necessary to have high intensity pulses, and the only way to separate thermal mechanisms from the electronic mechanisms is to use very short pulsewidths (<100 fs). This has been done successfully by several groups, and brings up the role of large amounts of sub-vacuum electrons. The production of potentially large numbers of highly reactive sub-vacuum and above-vacuum photoelectrons also needs to be considered in this problem because these electrons have been shown to efficiently interact with adsorbate molecules,[9,12–17] The present work characterizes this aspect of the photophysical processes operating at the surface, which may also contribute to the surface photochemistry.

EXPERIMENT

The laser system used in these studies consists of a self-mode-locked Ti:Sapphire laser pumped by about 7.7 W from a cw Ar^+ laser. This system produces pulses with energy of about 10 nJ/pulse, with a pulsewidth of 70–90 fs at a repetition rate of 82 MHz, and is tunable from 750 to 850 nm. Pulse broadening due to the group velocity dispersion of the uncompensated pulse as it passes through focusing lenses and the chamber window leads to a pulse width of roughly 100 fs at the sample. Some of the results presented here required the use of a regenerative amplifier utilizing chirped pulse amplification.[18] The amplifier is pumped by an intracavity doubled YLF laser operating at a repetition rate of 1 kHz that provides about 3 W of pump power. The output of the regenerative amplifier is about 400 μJ/pulse before recompression, and 180 μJ/pulse after recompression, and the pulse width is roughly 200 fs after recompression for the studies performed here.

The ultrahigh vacuum system uses standard techniques to achieve a base pressure of 2×10^{-10} Torr. Our Cu(110) and Cu(100) samples were cleaned by heating in oxygen to remove bulk carbon impurities and then further cleaned by repeated sputter-annealing cycles. We chose Cu because its electronic structure is relatively simple, and has been well studied. In addition, the laser photon energy of 1.6 eV is too small to excite either *d*-band electrons or image states by a one photon process, which might otherwise complicate the interpretation of the results. The work function of Cu(110) is 4.5 eV, and that for Cu(100) is 4.6 eV. In either case, at least three photons are required to produce photoemission since the photon energy is 1.6 eV. The Cu sample is mounted on a manipulator with five degrees of freedom that allows a variety of angles of incidence of the laser and detector angles to be investigated. The photoelectron spectra were measured with a 10 cm inner radius hemispherical energy analyzer with 1% relative energy resolution and a 10° acceptance angle. The data reported here, with the exception of the polarization dependence study, were obtained with the surface normal parallel to the axis of the detector entrance, and the laser beam making a 45° angle with the surface normal. The crystallographic [010] direction lies in the plane defined by the laser beam and the surface normal. Transmission energies of either 10 or 20 V were used, which leads to 100 or 200 meV resolution, respectively. A -3.0 to 6.0 V bias is applied to the sample to eliminate the effects of any stray electric fields. The applied bias voltage extends the range of **k** states being collected, but contributes less than 0.11 eV uncertainty to the energy resolution since the bias is small and copper exhibits nearly free electron behavior. The electron kinetic energies reported here have the kinetic energy due to the bias voltage subtracted, and correspond to the kinetic energy of the photoemitted electrons leaving the metal surface.

RESULTS

A schematic representation of the photoexcitation with the laser fundamental, second harmonic, and third harmonic is shown in Fig. 1. The measured spectra when using the three different photon energies are shown in Fig. 2. The lowest photon energy, shown as $h\nu_1$ corresponds to the fundamental laser wavelength at roughly 770 nm, or about 1.6 eV. Photon energies $h\nu_2$ and $h\nu_3$ are obtained by doubling and tripling the laser fundamental, respectively. Given the 4.5 eV work function of Cu(110), it is seen in Fig. 1 that photoemission requires three photons at the laser fundamental, or two doubled photons, or one tripled photon.

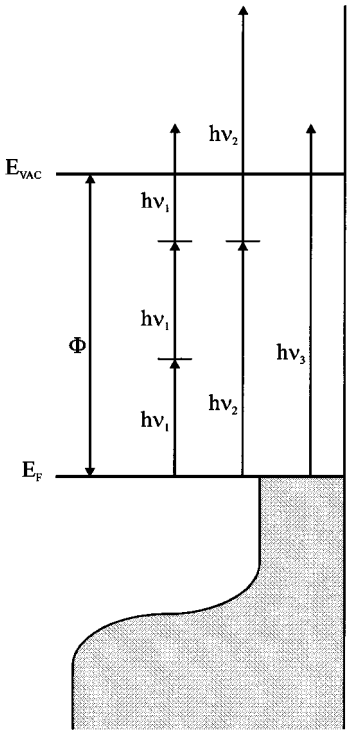

FIG. 1. Schematic representation of one-, two-, and multiphoton photoemission spectra from copper. The photon energy of the laser fundamental is $h\nu_1$, and that for the second and third harmonics is $h\nu_2$, and $h\nu_3$, respectively, and Φ is the work function.

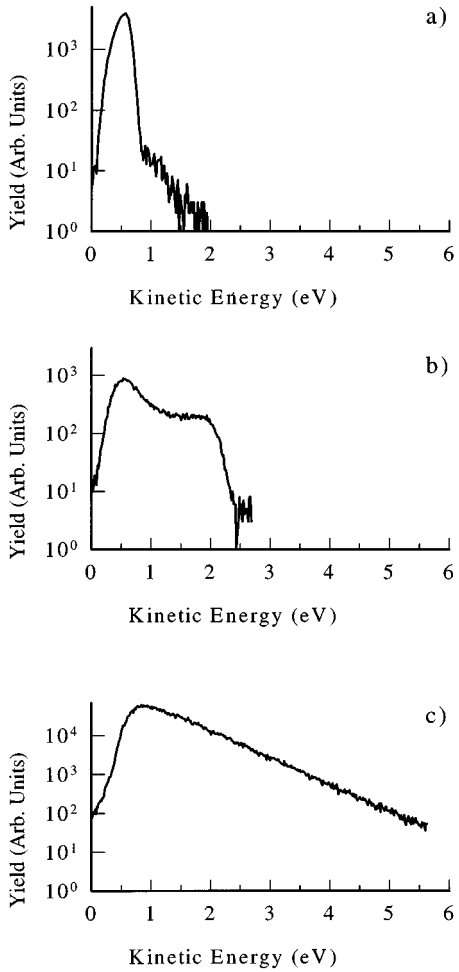

FIG. 2. One-photon, two-photon, and multiphoton photoemission spectra from Cu(110). (a), (b), and (c) are the spectra measured when using photon energies of $h\nu_3$, $h\nu_2$, and $h\nu_1$, respectively, as shown in Fig. 1. The peak laser intensities at $h\nu_3$, $h\nu_2$, and $h\nu_1$, are 1×10^4 W/cm^2, 1×10^7 W/cm^2, and 1×10^9 W/cm^2.

The cases of one photon and two photon photoemission are in complete accordance with expectations, as seen in Figs. 2(a) and 2(b). That is, the width of the photoemission spectrum is given by the total photon energy minus the work function. The behavior is completely different in the case in which the laser fundamental is used. In particular, rather than dropping off at the point in energy where three photons have been absorbed, the kinetic energy of the photoelectrons extends 6–8 eV above the vacuum threshold. There are electrons being emitted whose kinetic energy would correspond to the absorption of over seven photons. Studies of the laser power dependence of the photoemission yield indicate that the yield as a function of electron kinetic energy does *not* follow a power law based on the number of photons that correspond to the kinetic energy of the emitted electron, as seen in Fig. 3(b).

As the sample is moved around normal to the direction of electron emission, hot spots are found at which the photoemission yield increases dramatically, on the order of a factor of 100–1000. These hot spots are much smaller than the laser beam waist at the sample. This was determined by translating the sample from side to side and measuring the distance from 10% of the maximum photoemission yield on one side of the maximum, through the maximum itself, and to 10% of the maximum on the other side. Given that the signal varies with the third power of the laser intensity, the 10% points occur at roughly 50% maximum laser intensity. We measured a distance of 96 ± 15 μm as the distance between a 10% photoemission yield on either side of the maximum. The beam waist (the diameter of the $1/e^2$ points) at the sample surface is measured to be about 100 μm through measurements with pinhole apertures which indicates a full width at half maximum (FWHM) of roughly 60 μm, and yields an 85 μm projection on the surface since it is at a 45° angle relative to the laser beam. These measurements place an upper limit on the size of the hot spots and are consistent with roughness features that are far smaller than the laser beam spot size.

Polarization studies were carried out on the Cu(100) sample that support the interpretation of these results in terms of locally rough hot spots. Since *p*-polarized light is more strongly absorbed than *s*-polarized light, it is necessary to rotate the sample into an orientation normal to the laser beam in order to prevent the polarization-dependent absorbtivity from affecting the polarization dependence studies. This causes the sample to be oriented at 45° relative to the detector entrance and slightly lowers the absolute intensity of the signal, but it does not affect the relative intensities of the spectra obtained. The polarization was rotated with a half-

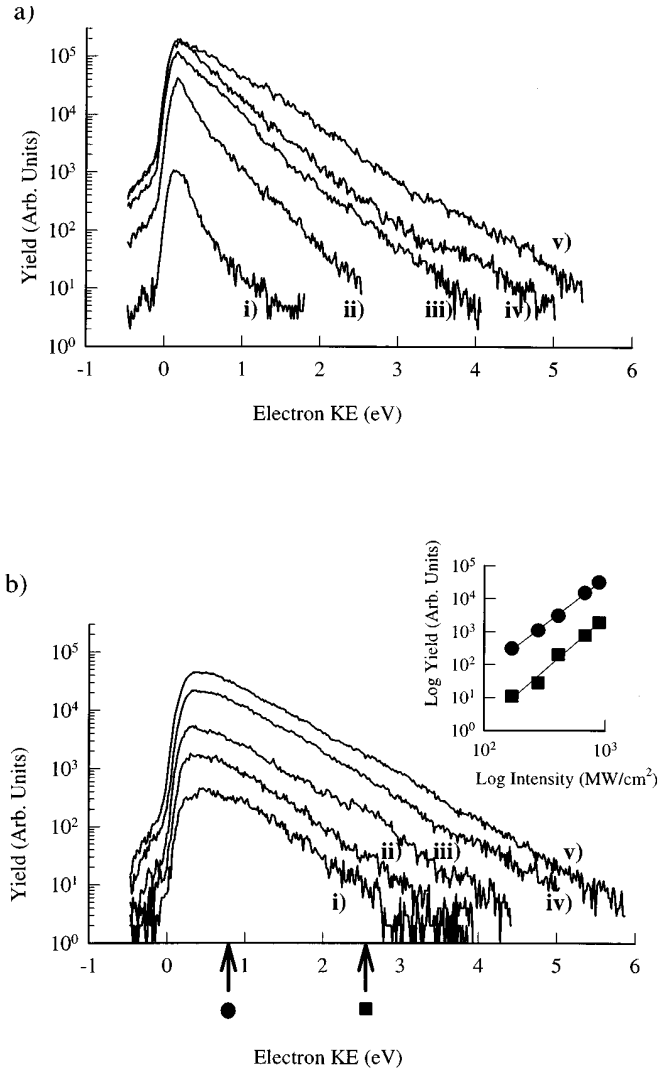

FIG. 3. Typical spectra as a function of laser intensity. The intensity dependence shown in (a) and (b) are each obtained for about 50% of the hot spots. The laser intensities employed for the five curves are (i) 0.17 GW/cm^2, (ii) 0.28 GW/cm^2, (iii) 0.41 GW/cm^2, (iv) 0.68 GW/cm^2, (v) 0.89 GW/cm^2. The inset in b displays a log–log plot of the photoelectron yield vs the laser intensity taken while monitoring 0.8 eV electron kinetic energy (solid circles) and 2.5 eV electron kinetic energy (solid squares). The slope of the log–log plot at 0.8 eV is 2.8 and the slope at 2.5 eV is 3.2.

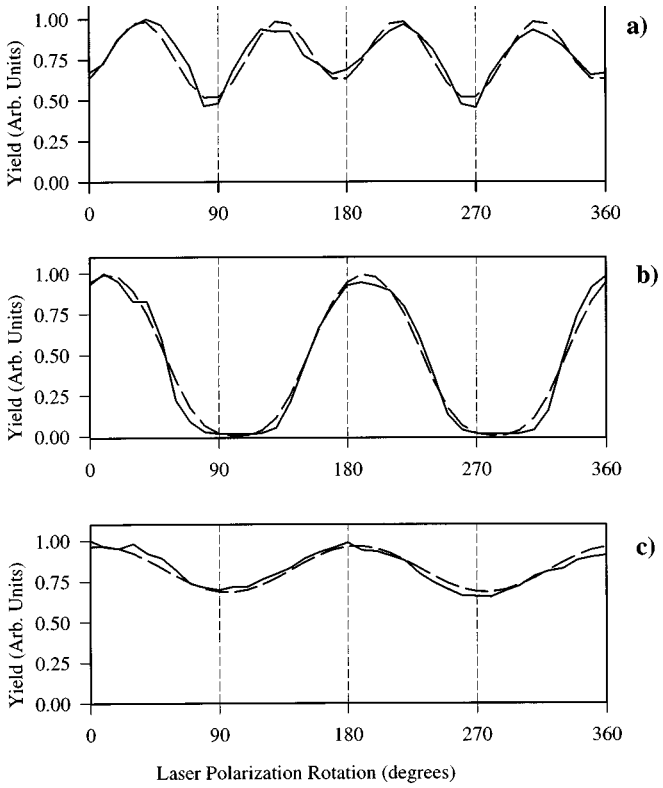

FIG. 4. The solid lines indicate the polarization dependence of three hot spots. A half-wave plate was rotated through 180° in order to rotate the laser polarization through 360°. The laser polarization is along the crystallographic [010] direction at 0°, 180°, and 360°. The dashed lines are the calculated polarization dependencies using Eq. (1) and the quantities in Table I.

wave plate such that the position of the beam on the surface did not change. It is found that the signal has a twofold symmetry as a function of polarization rotation. That is, that maxima (and minima) are separated by 180° of polarization rotation, but the maxima and minima are not necessarily aligned with the crystallographic axes. Furthermore, if the crystallographic axes were significantly affecting the signal level, there would be horizontal *and* vertical maxima, where the fourfold symmetry reflect the underlying fcc lattice along the [100] direction. There are also secondary maxima and minima as a function of polarization rotation at more or less arbitrary polarization. Sometimes hot spots are found that have maxima with vertical polarization, sometimes with horizontal polarization, and sometimes at intermediate positions, all with equal probability. This indicates that the rough spots destroy the order at the near-surface region, and when the light couples into the hot spot it is not affected by the underlying crystallographic symmetry several tens of Å away. Figure 4 shows the polarization dependence of the photoelectron yield for three different hot spots. The solid lines are the measured data, and the dashed lines are the results of fitting the observed normalized yields to the following functional form:

$$Y = A_1 \cos^{2n}(\theta - \phi_1) + A_2 \cos^{2n}(\theta - \phi_2) + C, \tag{1}$$

the yield is given by Y. The coefficients A_1 and A_2 determine the maximum contribution from the $\cos^{2n}(\theta-\phi)$ terms, θ is the amount of rotation of the laser polarization, in degrees, ϕ_1 and ϕ_2 are the phases for each contribution, also in degrees. A constant offset is specified by C. The $\cos^{2n}(\theta-\phi)$ angular dependence was chosen to describe a dipole excitation mechanism with an intensity dependence that varies as the laser intensity taken to the nth power. The parameters for each of the curves in Fig. 4 are given in Table I. It is expected that n should be 3 if the yield depends on the laser intensity cubed, as is shown in the inset of Fig. 3(b). This, in fact, provides a reasonable fit in Figs. 4(a) and 4(b), but not Fig. 4(c). The purpose of plotting the polarization dependence is to demonstrate the varied responses for different

TABLE I. Parameters used to fit the curves in Fig. 4 to the functional form shown in Eq. (1). The coefficients A_1 and A_2 were constrained to be equal in parts (a) and (b).

Curve	A_1	A_2	ϕ_1	ϕ_2	n	C
Figure 4(a)	0.58	0.58	36	134	3	0.41
Figure 4(b)	0.72	0.72	32	173	3	0.00
Figure 4(c)	0.28	⋯	6	⋯	1	0.68

roughness features rather than perform a detailed, quantitative analysis of the functional form that best describes the polarization dependence.

The twofold symmetry arises because the laser polarization has twofold symmetry and there is a strong, yet randomly oriented, polarization dependence for any given hot spot that is not related to the underlying crystal axes. The polarization dependence of a roughness feature arises from the fact that this is a nonlinear process, and if the light preferentially couples into a certain orientation on the roughness feature, then there will be a strong enhancement when the polarization is rotated into that particular orientation. The maxima at other angles and the offset from zero seen at some hot spots could be due to several roughness features with different orientations that are very close to each other, or a single roughness feature that happens to be able to efficiently absorb light of a variety of polarizations.

We find that the occurrence of hot spots is increased when the sample is not annealed after sputtering. It is known that sputtering roughens the surface on a nanometer scale,[19] and this results in a higher probability of finding surface defects for better coupling of the laser field to the surface plasmons (see the following). There is a roughly tenfold increase in the number of hot spots per unit area, and the emission from the hot spots is slightly higher (about a factor of 2–5) when the sample is not annealed compared to when it is.

Semilogarithmic plots of the spectra as a function of laser intensity for two different spots are shown in Fig. 3. Two types of intensity dependent behavior are observed. Spectra similar to Fig. 3(a), where the slope changes as the laser intensity increases, are obtained about half the time, while the other half of the time the slope is constant as the laser intensity is increased, as shown in Fig. 3(b). The inset in Fig. 3(b) displays a log–log plot of the photoemission yield vs laser intensity at the two different electron kinetic energies indicated with the arrows. The fact that the slopes on the log–log plot are the same indicates the same power dependence at high kinetic energy as at low kinetic energy, even though an additional photons' worth of energy is absorbed. In the perturbative limit of multiphoton processes, the slope of a log–log plot of signal vs laser intensity will yield the number of photons involved in the process. Clearly, a perturbative description of the photoemission is incorrect, and this is exactly analogous to observations of ATI or TI in the gas phase.[3,4]

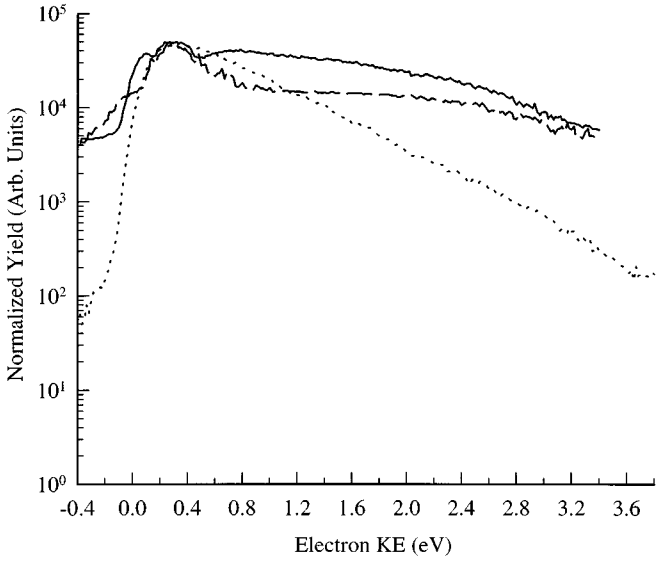

FIG. 5. The effects of space charge are clearly seen as the laser intensity is increased from 1.0×10^9 (dotted line) to 2.6×10^{10} (dashed line) to 1.2×10^{11} W/cm^2 (solid line). As space charge effects become greater, a bulge develops in the high energy portion of the spectrum.

DISCUSSION

It is necessary to first rule out three possible mechanisms that might be thought to produce the observed spectra before discussing the underlying cause of these observations. First, the possibility of space charge effects needs to be ruled out. It is known that electrons that are confined to a small region in vacuum will all mutually repel each other due to the Coulombic repulsion, that is, space charge. We show that the space charge effect is not affecting our results. Petite and co-workers showed both theoretically and experimentally that if roughly 10 000 electrons are generated in a region the diameter of the laser beam (100 μm) that is roughly 10 μm thick, that they can reach kinetic energies on the order of 2–4 eV.[8] We have measured roughly 1 pA of current drawn through the sample when using moderate laser intensity (1×10^8 W/cm^2), which corresponds to less than 0.1 electron being emitted per laser pulse, and, therefore, completely eliminates the possibility of space charge effects from affecting our measurements. Furthermore, when employing the regenerative amplifier, we can increase the power per pulse by up to four orders of magnitude if desired. Figure 5 clearly shows the onset of space charge effects on the photoemission spectrum. The lower curve corresponds to that obtained at maximum intensity with the unamplified system, while the upper two curves demonstrate the measurable effects of space charge at one and two orders of magnitude higher intensity. At these higher laser intensities, the spectrum becomes distorted and develops a notable bump at higher kinetic energy. The fact that these distortions do not occur until a factor of 10 above the maximum intensity used in the studies with the unamplified laser provides further evidence that we do not need to consider space charge effects on the observed photoemission spectrum when not using the amplified laser system.

The enhanced yield of photoelectrons at higher laser intensity also needs to be considered. As seen from Fig. 5, for amplified laser conditions which approach the intensities of typical photodesorption experiments, the number of photoemitted electrons is significant enough to produce space charge effects. In this process, some electrons are accelerated toward the detector with higher energy, while an equal number are simultaneously accelerated back toward the surface and do not escape the surface region.[20] These latter electrons would be available for inducing desorption processes through well known electron induced desorption mechanisms, i.e., electron attachment leads to a large amount of vibrational energy in the adbond.[12,13,15,17] The present study indicates such a process could be occurring under the intense laser excitation conditions typically employed. An important consideration is the relative contribution of photoemitted electron-induced desorption relative to other proposed mechanisms. This issue is an important one which needs to be resolved because photoemitted electrons offer an alternative, and to a certain extent, simple explanation for the nonlinear yields of hot desorption products observed in femtosecond laser studies of metal surfaces.

Next, the possibility of thermionic emission is ruled out. Thermionic emission results when the high energy tail of the Fermi–Dirac distribution of a hot, thermalized electron distribution extends above the vacuum level. For intense optical pulses of duration shorter than the electron–photon energy relaxation time (a few ps), a large thermal nonequilibrium between the electrons and phonons can be achieved due to the much smaller heat capacity of the electrons. If the photoelectron spectra measured here were to represent the high energy tail of a hot Fermi–Dirac distribution, the photoelectron yield would be proportional to $e^{-E/kT}$ and the slope of the semilogarithmic plots in Fig. 3(b) would yield the underlying electronic temperature. The slopes in Fig. 3(b) would then indicate an electronic temperature of about 7000 K, which is far too high, given our laser pulse energy of less than 100 nJ/cm^2/pulse and the heat capacity of copper. A second method to rule out the possibility of thermionic emission is to perform a time resolved experiment using the pump–probe technique. We find that the photoelectron yield as a function of pump–probe delay is identical to the third order autocorrelation function of the laser pulse as shown in Fig. 6(a), i.e., the photoelectron yield is determined solely by the cube of the instantaneous laser intensity which is consistent with the slope of three in the inset of Fig. 3(b). If transient electronic heating was occurring, then the full width at half-maximum of this pump–probe experiment would be larger than the FWHM of the third order autocorrelation because the elevated electronic temperature persists for several hundred femtoseconds or longer, as measured by other workers using amplified femtosecond laser systems.[21,22] Figure 6(b) presents the results of the calculated temperature rise[23] of the electron distribution for our experimental conditions. For simplicity, the electronic heat capacity was held fixed at 3.3×10^4 JK/m^3, rather than letting it be linearly dependent on temperature, thus, the calculated electronic temperature rise will actually be overestimated. A thermal conductivity of 80 WK/m was used, and the peak laser intensity, pulse duration (FWHM), and spot size were 9×10^8 W/cm^2, 100 fs, and 100 μm, respectively. The reflectivity and absorption coefficient were 0.5 and 79 μm^{-1}, respectively. The electronic temperature and lattice temperature were not coupled to each other for this calculation because it is known that the timescale for energy relaxation from electronic excitation into the lattice takes place on a time scale of 1–3 ps,[24] which is much longer than the timescale of interest for this calculation. The results of this calculation show that the maximum temperature will be roughly 700 K, which is far lower than a temperature of 7000 K which would be required for a thermal distribution of electrons to produce the measured photoemission spectra (see the aforementioned). More importantly, if a thermal mechanism was responsible for the observed electronic distribution, the temperature would remain elevated for well over a picosecond, which clearly does not agree with the pump–probe measurements.

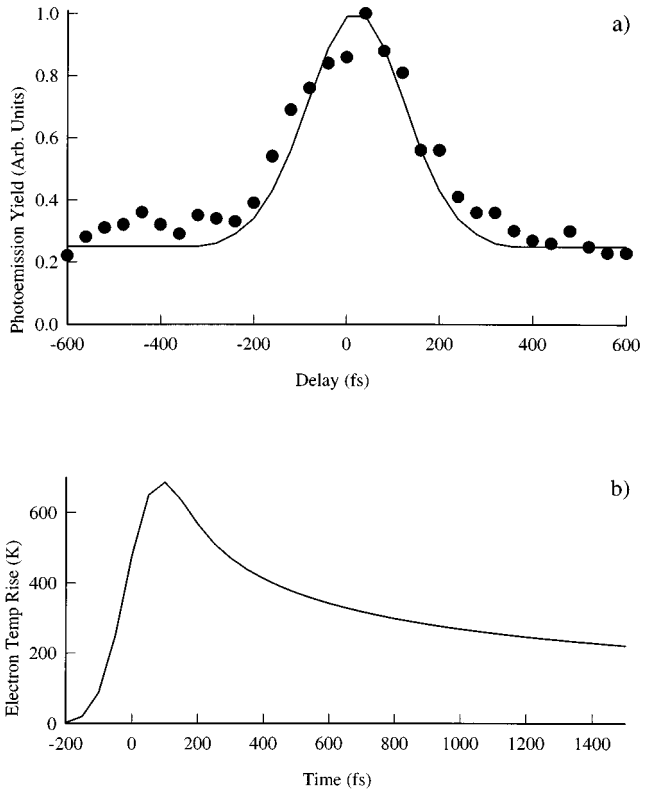

FIG. 6. (a) displays the photoemission yield as a function of delay time between two equal intensity pulses (solid circles) using the amplified laser with a 190 fs pulsewidth. The amplified laser was employed because a 2–3 mm beam diameter could be used, and it was not necessary to search for hot spots. The solid line is the calculated third order autocorrelation function for a Gaussian pulse with a 190 fs FWHM. (b) is the calculated electronic temperature rise of the sample when using the unamplified laser.

Finally, the possible effect of the laser field itself on the photoemitted electron energy spectrum needs to be considered. It is known that an electron that is in a very intense laser field will acquire kinetic energy as it is pushed out of the region of high laser intensity to low intensity. This effect is known as ponderomotive acceleration[4] and arises from the Gaussian spatial distribution of the laser beam. The action of

the spatial intensity gradient is not instantaneous because the electrons must travel a distance on the order of the laser spot size to acquire kinetic energy due to acceleration from this gradient. For laser pulses shorter than one ps in duration, there is simply not enough time for the electron to gain a significant amount of kinetic energy before the laser pulse has ended.[3] Therefore, this mechanism cannot account for the observed behavior of the photoelectrons.

As discussed in the Introduction, ATI or TI in the gas phase requires laser intensities on the order of 10^{14} W/cm^2, whereas the photoemission that we are measuring occurs at only 10^8 W/cm^2. The fact that the photoemission occurs at a metal surface, and that it depends on hot spots or surface roughness, reconciles these two seemingly contradictory observations. It is well known that a tremendous enhancement of the electric field at the roughened surface of a metal can be achieved through excitation of surface plasmons.[25] The excitation of surface plasmons by photons is forbidden at a smooth surface/vacuum interface, because it is not possible to simultaneously conserve energy and wave vector for both the photon and surface plasmon.[25] The most common way to overcome this obstacle is to deposit a thin metal film on a dielectric substrate, such as a quartz prism, and direct the light through the dielectric medium rather than through vacuum. This allows direct coupling of photons and surface plasmons, and is known as the attenuated total reflection (ATR) method.[25] A second method to couple photons and surface plasmons is to rule a grating on the surface. In this case, the photon wave vector and surface wave vector need not be equal; efficient coupling can be achieved whenever the difference between the photon and surface plasmon wave vectors are integral multiples of $2\pi/a$, where a is the grating constant. In the present study a randomly roughened surface is used, which can be described in terms of its Fourier components of a two-dimensional grating, and will thus be able to couple photons and surface plasmons over a wide range of difference in wave vectors.[25,26] In addition to providing a coupling mechanism, surface roughness features can also serve to localize and further enhance the surface plasmons.[25,26]

We deliberately roughened the surface to determine its effect on the photoemission yield. The sample was sputtered with Ar^+ ions at kinetic energies from 1 to 3 kV, at 1×10^{-6} Torr background pressure for 20 min. Girard *et al.* have performed scanning tunneling microscope studies of a Cu(100) surface after sputtering with 0.6 kV Ar^+ ions, and found roughness features on a 5–20 nm scale that are on the order of 1 nm deep.[19] The higher energy Ar^+ ions used in the present study will more effectively roughen the surface, leading to features that are the optimum size to maximize the localized surface plasmon fields.[25,26] Studies of surface enhanced Raman spectroscopy, or SERS, found that the Raman yield could be increased by up to 6 orders of magnitude at a roughened silver surface.[26] Moskovits discusses SERS and reasons for the enhancement, and concludes that the largest contribution to the enhancement is due to coupling of the photons with surface plasmon modes *via* random surface roughness, as described earlier. In order to increase the SERS yield by six orders of magnitude, the electric field would have to be enhanced by three orders of magnitude.

Based on these comparisons with previous work, the surface roughness encountered at the hot spots can increase the electric field enough to cause either ATP or TI. In atomic physics, the reason for the loss of the ATI structure at higher laser energies is tunneling. The electrons interact with the superposition of the Coulomb potential and the laser induced electromagnetic field. The maximum of this potential decreases steadily as the laser field increases. At a critical laser intensity, the electron can periodically tunnel into the vacuum as a result of the oscillating laser electric field. In the description of Corkum *et al.*,[27] the electron escapes with very little excess velocity and then behaves as a free particle in the laser field. The relevant quantity γ is proportional to the ratio of the laser frequency ω to the electromagnetic field strength E:

$$\gamma=\sqrt{\frac{I_P}{2U_P}}=\frac{\omega}{E}\cdot\frac{\sqrt{2mI_P}}{e}, \tag{2}$$

where I_P is the ionization potential of the atom, U_p is the ponderomotive potential, m is the electron mass, and e is the electron charge. This ratio is known as the adiabaticity, or Keldysh parameter and is essentially the ratio of the laser frequency ω to the tunneling frequency ω_t.[4] The parameter γ is generally used to separate the multiphoton mechanism ($\gamma\gg1$) from the tunneling ($\gamma\ll1$) regime.

Using 110 ps long laser pulses with intensities up to 120 GW/cm^2, Toth *et al.* used photoyield measurements to show that a transition of pure multiphoton to optical tunneling may also occur at a gold surface.[28] However, that experiment was done in the long pulse regime ($t>80$ ps) where ponderomotive acceleration and space charge broadening can influence the photoemission spectrum. In contrast to ATP, tunneling is not expected to lead to discrete steps characterized by a width equal to one photon energy. The electron kinetic energy distribution will instead be smeared out due to a spread in the initial time of tunneling, relative to both the phase of the laser field and the instantaneous intensity of the field at the time of emission.[3] This view is supported by the recent measurement of Mevel *et al.*[29] who found strikingly similar behavior to this work for multiphoton ionization of noble gas atoms.

Optical tunneling from metals surfaces is more complicated than from single atoms. The Keldysh parameter γ depends critically on the local electromagnetic field strength, which in our case is significantly enhanced by the coupling of the laser light into surface plasmons. Tunnel emission studies performed with static fields show that roughly 5–10 V/Å (10^{11} V/m) is required to allow electrons to tunnel into the vacuum, which would require a laser intensity of 1×10^{15} W/cm^2. The laser intensity used in the present studies is 10^7–10^9 W/cm^2 which provides 10^7–10^8 V/m.[30] Therefore, it is the surface roughness that provides the additional two to three orders of field enhancement with a concomitant four to six orders of magnitude intensity enhancement, which is consistent with previous SERS studies utilizing roughened surfaces.

SUMMARY

We have measured photoelectrons with far more kinetic energy than would be expected based on the work function of the sample and photon energy used. These results are unique in that they are obtained at lower intensity than similar gas phase studies and other above threshold photoemission studies from metals. The role of surface roughness, or defects, is seen to be critical in this process. It should be noted that the production of photoelectrons possessing large amounts of kinetic energy when employing photon energies well below the work function has important implications with respect to photodesorption studies carried out with intense laser pulses. One of the reasons that these results are important is that there are several groups investigating ultrafast desorption of adsorbates from metal surfaces driven by subvacuum hot electrons using high intensity femtosecond lasers.[11,31–34] Furthermore, there are other groups that observe desorption driven by electrons photoemitted from a surface using ultraviolet light at very low intensities, indicating that it is the electron kinetic energy, not the number of excited electrons that drives many surface photoinduced processes.[9,13,16,17]

The present study measures electrons with significant amounts of kinetic energy that are generated with photon energies well below the photoemission threshold using laser intensities at or below those used in many photodesorption experiments. Future studies will address whether multiphoton photoelectrons with excess kinetic energy or space charge effects at high fluence make a contribution to the photodesorption yield measured in the ultrafast photodesorption experiments.

The use of a high repetition rate, low pulse energy, ultrafast laser system has allowed data to be obtained that is free of ambiguities due to thermal heating of the sample (either electrons or lattice), space charge effects, or ponderomotive acceleration. Furthermore, the laser intensities used here are well below those required to produce above threshold phenomena in the gas phase, and the roughness of surface defects provides the requisite field enhancement at the surface. More important, however, is the fact that we have been able to measure photoelectrons with excess kinetic energy from copper surfaces with very low pulse energy, intensity, and duration, leading to a measurement that is free of contributions from competing processes that are present in earlier studies.

ACKNOWLEDGMENTS

The authors would like to thank R. Grobe and H. H. Eberly for several helpful discussions. The authors would also like to thank J. C. Déak for technical assistance. This work was carried out under the National Science Foundation Grant No. CHE-9120001.

[1] P. Agostini and F. Fabre, Phys. Rev. Lett. **42**, 1127 (1979).
[2] G. G. Paulus, W. Nicklich, H. Xu, P. Lambropoulos, and H. Walther, Phys. Rev. Lett. **72**, 2851 (1994).
[3] R. R. Freeman and P. H. Bucksbaum, J. Phys. B **24**, 325 (1991).
[4] J. H. Eberly, J. Javanainen, and K. Rzazewski, Phys. Rep. **204**, 331 (1991).
[5] W. S. Fann, R. Storz, and J. Bokor, Phys. Rev. B **44**, 10980 (1991).
[6] S. Luan, R. Hippler, H. Schwier, and H. O. Lutz, Europhys. Lett. **9**, 489 (1989).
[7] G. Farkas, C. Tóth, and A. Kóházi-kis, Opt. Eng. **32**, 2476 (1993).
[8] G. Petite, P. Agostini, R. Trainham, E. Mevel, and P. Martin, Phys. Rev. B **45**, 12210 (1992).
[9] X.-L. Zhou, X.-Y. Zhu, and J. M. White, Surf. Sci. Rep. **13**, 76 (1991).
[10] F. M. Zimmermann and W. Ho, J. Chem. Phys. **100**, 7700 (1994).
[11] F. Budde, T. F. Heinz, A. Kalamarides, M. M. T. Loy, and J. A. Misewich, Surf. Sci. **283**, 143 (1993).
[12] M. Asscher, F. M. Zimmermann, L. L. Springsteen, P. L. Houston, and W. Ho, J. Chem. Phys. **96**, 4808 (1992).
[13] F. Weik, A. de Meijere, and E. Hasselbrink, J. Chem. Phys. **99**, 682 (1993).
[14] J. W. Gadzuk and C. W. Clark, J. Chem. Phys. **91**, 3174 (1989).
[15] J. W. Gadzuk, L. J. Richter, S. A. Buntin, D. S. King, and R. R. Cavanagh, Surf. Sci. **235**, 317 (1990).
[16] E. P. Marsh, M. R. Schneider, T. L. Gilton, F. L. Tabares, W. Meier, and J. P. Cowin, Phys. Rev. Lett. **60**, 2551 (1988).
[17] Z. J. Sun, S. Gravelle, R. S. Mackay, X. Y. Zhu, and J. M. White, J. Chem. Phys. **99**, 10021 (1993).
[18] G. Mourou and D. Umstadter, Phys. Fluids B **4**, 2315 (1992).
[19] J. C. Girard, Y. Samson, S. Gauthier, S. Rousset, and J. Klein, Surf. Sci. **302**, 73 (1994).
[20] T. L. Gilton and J. P. Cowin, J. Appl. Phys. **68**, 4802 (1990).
[21] J. G. Fujimoto, J. M. Liu, E. P. Ippen, and N. Bloembergen, Phys. Rev. Lett. **53**, 1837 (1984).
[22] X. Y. Wang, D. M. Riffe, Y.-S. Lee, and M. C. Downer, Phys. Rev. B (to be published).
[23] J. H. Bechtel, J. Appl. Phys. **46**, 1585 (1975).
[24] H. E. Elsayed-Ali, T. Juhasz, G. O. Smith, and W. E. Bron, Phys. Rev. B **43**, 4488 (1991).
[25] H. Raether, *Surface Plasmons on Smooth and Rough Surfaces and on Gratings*, Springer Tracts in Modern Physics (Springer, New York, 1988), Vol. 111.
[26] M. Moskovits, Rev. Mod. Phys. **57**, 783 (1985).
[27] P. B. Corkum, N. H. Burnett, and F. Brunel, Phys. Rev. Lett. **62**, 1259 (1989).
[28] C. Tóth, G. Farkas, and K. L. Vodopyanov, Appl. Phys. B **53**, 221 (1991).
[29] E. Mevel, P. Breger, R. Trainham, G. Petite, P. Agostini, A. Migus, J. P. Chambaret, and A. Antonetti, Phys. Rev. Lett. **70**, 406 (1993).
[30] W. H. Flygare, *Molecular Structure and Dynamics* (Prentice–Hall, Englewood Cliffs, NJ, 1978).
[31] J. A. Prybyla, H. W. K. Tom, and G. D. Aumiller, Phys. Rev. Lett. **68**, 503 (1992).
[32] J. A. Misewich, A. Kalamarides, T. F. Heinz, U. Höfer, and M. M. T. Loy, J. Chem. Phys. **100**, 736 (1994).
[33] F. J. Kao, D. G. Busch, D. Cohen, D. Gomes da Costa, and W. Ho, Phys. Rev. Lett. **71**, 2094 (1993).
[34] F. Budde, T. F. Heinz, M. M. T. Loy, J. A. Misewich, F. de Rougemont, and H. Zacharias, Phys. Rev. Lett. **66**, 3024 (1991).